International Journal of Solids and Structures 47 (2010) 759–767

Contents lists available at ScienceDirect

International Journal of Solids and Structures

journal homepage: www.elsevier.com/locate/ijsolstr

On the singularities of a constrained (incompressible-like) tensegrity-cytoskeleton model under equitriaxial loading

Athanassios P. Pirentis, Konstantinos A. Lazopoulos *

Department of Mechanics, Faculty of Applied Mathematical and Physical Sciences, National Technical University of Athens, 5 Heroes of Polytechnion Av., Post Code 157 73, Zografou Campus, Athens, Greece

ARTICLE INFO

Article history:
Received 31 December 2008
Received in revised form 18 October 2009
Available online 22 November 2009

Keywords:
Tensegrity
Cytoskeleton
Singularity theory
Bifurcation
Stability
Constraints

ABSTRACT

Singularity theory is applied for the study of the characteristic three-dimensional tensegrity-cytoskeleton model after adopting an incompressibility constraint. The model comprises six elastic bars interconnected with 24 elastic string members. Previous studies have already been performed on non-constrained systems; however, the present one allows for general non-symmetric equilibrium configurations. Critical conditions for branching of the equilibrium are derived and post-critical behaviour is discussed. Classification of the simple and compound singularities of the total potential energy function is effected. The theory is implemented into the cusp catastrophe for the case of one-dimensional branching of the buckling-allowed tensegrity model, and an elliptic umbilic singularity for compound branching of a rigid-bar model. It is pointed out that singularity studies with constraints demand a quite different mathematical approach than those without constraints.

1. Introduction

The concept of tensegrity was initially apprehended and materialized in the sculptures of the artist Kenneth Snelson in 1948 and later patented by the architect R. Buckminster Fuller as a new method for designing geodesic structures (Fuller, 1961). Tensegrities are reticulated structures forming a highly geometric combination of bars and strings in space. In fact, tensegrity is a portmanteau word for "tension-integrity" referring to the integrity of structures as being based in a synergy between balanced continuous tension (elastic strings) and discontinuous compression (elastic bars) components. Pre-existing tensile stress in the string members, termed prestress, is required even before the application of any external loading in order to maintain structural stability. There already exists an extensive literature regarding the mechanics and advanced mathematics used for the integral description of these structures (e.g., Roth and Whiteley, 1981; Motro, 1992; Connelly and Back, 1998; Skelton et al., 2002; Lazopoulos, 2005a; Pirentis and Lazopoulos, 2006; Williams, 2007). The principal characteristics of tensegrity architecture are: the fact that elastic bars bear compressive load whereas elastic strings bear tensional load; prestress provides structural stability (self-equilibrated system); structural rigidity is proportionate to prestress; and the manifestation of "action at a distance" (Stamenović, 2006).

Almost three decades ago, the hypothesis that the *cytoskeleton* (CSK) is organised according to the principles of tensegrity architecture was introduced (Ingber et al., 1981; Ingber and Jamieson, 1985). The CSK is the intracellular filamentous biopolymer network whose constant remodelling directly affects almost all functions of living cells (Suresh, 2007). In the course of several years an ever increasing number of experimental observations have established that adherent cell behaviour is controlled and determined by its physical deformation and, especially, the deformation of the CSK. In the cellular tensegrity model and in terms of cell physiology, elastic bars correspond to microtubules while elastic strings correspond to the actin and intermediate filaments network (Stamenović, 2006, and references therein for an excellent overview). It has been found that the aforementioned mechanical properties of tensegrity systems are characteristic of the CSK as well (Ingber, 1993, 1998, 2008; Volokh et al., 2000; Stamenović, 2006). Actually, some of these properties were initially predicted by the tensegrity model and were later verified in laboratory experiments as mechanical properties of the CSK (Ingber, 2008).

In a series of previous theoretical studies by the authors, several aspects and properties of tensegrity architecture and CSK modelling have been discussed (Lazopoulos, 2005a,b; Pirentis and Lazopoulos, 2006; Lazopoulos and Lazopoulou, 2006a,b). The particular tensegrity model of this study has been used time and again during the last two decades for the investigation of the application of tensegrity architecture in CSK mechanics (Ingber, 1993; Stamenović et al., 1996; Coughlin and Stamenović, 1997, 1998; Wendling et al., 1999; Volokh et al., 2000; Wang and Stamenović, 2000).

* Corresponding author.
E-mail address: kolazop@central.ntua.gr (K.A. Lazopoulos).

0020-7683/$ - see front matter © 2009 Elsevier Ltd. All rights reserved.
doi:10.1016/j.ijsolstr.2009.11.010

Appropriate modifications of the model have been presented in the literature in order to address specific problems from a broad range of phenomena related to the CSK (Stamenović, 2006; Ingber, 2008). However, previous studies by the authors and others did not take explicitly into account the fact that cells are almost incompressible. Here, motivated by this observation and in order to mimic cellular behaviour we integrated to the model a condition (constraint) that prohibits volumetric change, albeit, allows deformation.

In its initial unloaded configuration the tensegrity model under examination presents three-dimensional symmetry. Under the application of external equitriaxial loading and when the critical value is reached, the structure loses symmetry similarly to the case of Rivlin's cube (Rivlin, 1948, 1974; Ogden, 1997; Golubitsky et al., 1988). Two kinds of instabilities appear: the first is related to the global (overall) instability of the model and the second is due to local Euler buckling of the bars; both will be discussed later in the text along with the emergence of subsequent compound instabilities. The current tensegrity model, although simple, is a system with multiple degrees of freedom and presents a rich mechanical response that cannot be described in its entirety by force equilibrium concepts alone. To this end, an integral study of the model behaviour is effected by employing Singularity Theory for constrained systems – emerging from differential topology (Porteous, 1971, 1994). Even though formal branching theory demands such difficult tasks as the elimination of passive coordinates and the normalization of the total potential energy function (Thompson and Hunt, 1973; Vainberg and Trenogin, 1974; Troger and Steindl, 1991), the free coordinate bifurcation procedure elaborated here does not set these requirements. Applying the presented theory (Lazopoulos, 1994; Lazopoulos and Markatis, 1994), the various singularities of the total potential energy function exhibiting simple or compound branching of its equilibrium paths, under the influence of any constraints, can be investigated. In this formulation, explicit formulae of the critical conditions for branching are naturally derived and the classification of singularities provides the number and stability study of the post-critical equilibrium paths. The current treatment is an extension of previous work on the subject by including systems with constraints.

2. The tensegrity CSK model and its total potential energy function

The system under investigation comprises six inextensible elastic bars interconnected with a total of 24 elastic strings in the fashion shown in Fig. 1. Although the bars acquire an inextensible elastic curve, they may be buckled. In absence of external loading the initial geometrical configuration is dominated by prestress; specifically, the tensile forces carried by the strings are balanced by compression in the bars (Stamenović and Coughlin, 1999; Lazopoulos and Lazopoulou, 2006b).

In the initial configuration the self-equilibrated structure is fully symmetric and the origin of the Cartesian coordinate system is located in its centre. In fact, the three axes are aligned to the directions of the three pairs of parallel bars while the length of all string segments is the same. Following simple geometrical considerations it is straightforward to show that both the length of the string segments and the distance between the parallel bars are proportionate to the length of the bars (or, respectively, their chord-length if the bars are already buckled) (Kenner, 1976; Coughlin and Stamenović, 1997). The structure is subjected to a general three-dimensional loading such that forces of magnitude $T_X/2$, $T_Y/2$, $T_Z/2$ are applied at the endpoints of the bars (AA) and ($A'A'$), (BB) and ($B'B'$), (CC) and ($C'C'$), respectively (cf. Fig. 1). Thus, the parallel bars in each pair are either pulled apart or pushed towards each other, depending on whether the forces are

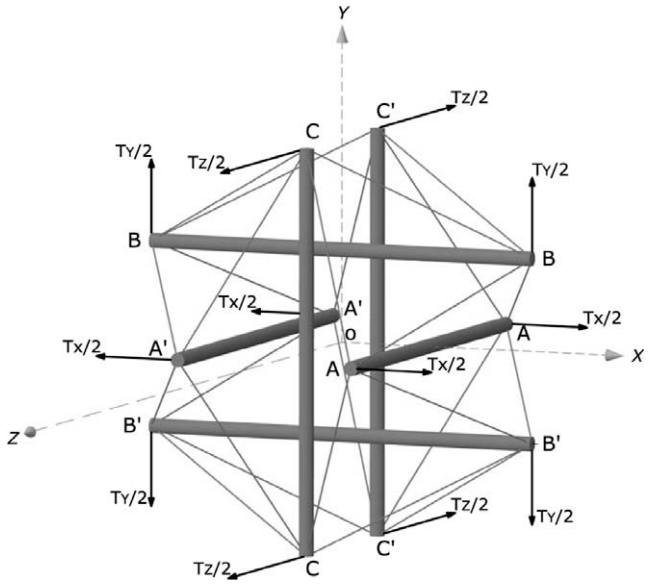

Fig. 1. Symmetric configuration of the tensegrity-cytoskeleton model.

extensive or compressive with respect to the overall system. Evidently, this results to a concerted change in all length values (current configuration). In the current configuration we call: s_X, s_Y, s_Z the distances between the parallel bars (or chord-lengths) (AA) and ($A'A'$), (BB) and ($B'B'$), (CC) and ($C'C'$), respectively; l_1 the length of the string segments (AB), ($A'B$), (AB'), ($A'B'$); l_2 the length of the string segments (AC), ($A'C$), (AC'), ($A'C'$); and l_3 the length of the string segments (BC), ($B'C$), (BC'), ($B'C'$). Then, simple geometrical arguments yield (Coughlin and Stamenović, 1997):

$$l_1 = \frac{1}{2}\sqrt{(L_2 - s_X)^2 + s_Y^2 + L_1^2}, \tag{1}$$

$$l_2 = \frac{1}{2}\sqrt{(L_1 - s_Z)^2 + s_X^2 + L_3^2}, \tag{2}$$

$$l_3 = \frac{1}{2}\sqrt{(L_3 - s_Y)^2 + s_Z^2 + L_2^2}, \tag{3}$$

where L_1, L_2 and L_3 are the current chord-lengths corresponding to the bars (AA) and ($A'A'$), (BB) and ($B'B'$),(CC) and ($C'C'$), respectively. If the deflection of the given buckled bar is defined by:

$$w_i(s) = \zeta_i \cdot \sin\left(\frac{\pi \cdot s}{L_0}\right), \quad i = 1,2,3, \tag{4}$$

where s and L_0 are the arc-length and length of the inextensible bar, respectively, and $\zeta_i \ll 1$, then the chord-length is expressed as:

$$L_i = L_0 - \frac{1}{2}\int_0^{L_0}\left(\left(\frac{dw_i(s)}{ds}\right)^2 - \frac{1}{4}\left(\frac{dw_i(s)}{ds}\right)^4\right)ds$$

$$\simeq L_0 - \frac{\pi^2 \cdot \zeta_i^2}{4L_0}, \quad i = 1,2,3. \tag{5}$$

Now, if ρ denotes the curvature radius, the non-linear curvature is approximated as:

$$\left(\frac{1}{\rho}\right)_i \simeq \frac{d^2 w_i(s)}{ds^2}\left(1 + \frac{1}{2}\left(\frac{dw_i(s)}{ds}\right)^2\right), \quad i = 1,2,3. \tag{6}$$

Hence, the strain energy of each buckled bar is expressed as:

$$Wb_i = \frac{1}{2}k_B\int_0^{L_0}\left(\frac{1}{\rho}\right)_i^2 ds \simeq \frac{k_B \cdot \pi^4 \cdot \zeta_i^2}{4L_0^3}, \quad i = 1,2,3, \tag{7}$$

where k_B is the bending stiffness of the bar. Regarding the string segments, we consider non-linear strain energy functions of the form:

$$W_j = \frac{1}{2!}k_1\left(\frac{l_j}{l_0}-1\right)^2 + \frac{1}{3!}k_2\left(\frac{l_j}{l_0}-1\right)^4 + \frac{1}{4!}k_3\left(\frac{l_j}{l_0}-1\right)^6, \quad j=1,2,3, \tag{8}$$

where parameters k_1, k_2, k_3 are elastic coefficients of the strings and l_0 is their rest length.

Summarizing the results of the analysis hitherto, it is evident that the strain energy of both bars and strings is a function of the arguments s_X, s_Y, s_Z, ζ_1, ζ_2, ζ_3. Hence, the total potential energy of the tensegrity model is now formulated as:

$$V = V(s_X, s_Y, s_Z, \zeta_1, \zeta_2, \zeta_3; T_X, T_Y, T_Z) = 2\sum_{i=1}^{3} Wb_i + 8\sum_{j=1}^{3} W_j - T_X \cdot s_X - T_Y \cdot s_Y - T_Z \cdot s_Z. \tag{9}$$

Further, in order to account for the incompressible material behaviour of cells, we impose the restriction to the system that the product of the distances between the parallel bars (or chord-lengths) is always kept constant, i.e., $s_X \cdot s_Y \cdot s_Z = \text{const}$. This is mathematically translated to the constraint:

$$f_1 = s_X \cdot s_Y \cdot s_Z - c = 0, \tag{10}$$

where c is the constant value.

3. Mathematical formulation and classification of singularities

Just for convenience, the notation of the arguments in Eq. (9) is changed in the fashion:

$$s_X = q_1, \quad s_Y = q_2, \quad s_Z = q_3, \quad \zeta_1 = q_4, \quad \zeta_2 = q_5, \quad \zeta_3 = q_6,$$
$$T_X = t_1, \quad T_Y = t_2, \quad T_Z = t_3.$$

Then the total potential energy function is rewritten in the equivalent form

$$V = V(q_m; t_n), \quad m = 1,\ldots,6 \text{ and } n = 1,2,3, \tag{11}$$

where q_m are the generalized coordinates and t_n the control parameters of the problem in hand, respectively. Therefore, the energy function is defined in the $(\mathbb{R}^6 \times \mathbb{R}^3)$ space. The generalized coordinates do not vary independently but are subjected to the constraint of Eq. (10).

The principle of virtual work demands that *for the state of equilibrium the work of the imposed forces be zero, for any infinitesimal variation of the system which is in harmony with the given kinematical constraints* (Lanczos, 1977).

Let us call the virtual generalized displacement vector dq_m an infinitesimal vector in the tangent space of the constraint manifold at an equilibrium point of the system. According to the principle of virtual work:

$$dV = \sum_{m=1}^{6}\left(\frac{\partial V}{\partial q_m}\right)\cdot dq_m = 0, \tag{12}$$

for any dq_m. It is recalled that the virtual generalized displacement vector should lie in the tangent space of the constraint manifold satisfying the equations:

$$df_p = \sum_{j=1}^{6}\left(\frac{\partial f_p}{\partial q_m}\right)\cdot dq_m = 0, \tag{13}$$

where p is the number of equations of the constraints; apparently, here $p = 1$. It is clear that the solutions dq_m of the system expressed by Eq. (13) should always satisfy the virtual work condition, Eq. (12). Therefore, Eqs. (12) and (13) have to be compatible; this means that they are linearly dependent. Consequently, there exists a vector:

$$\mathbf{a}' = [1 \;\; \eta_1], \tag{14}$$

such that the equations:

$$\frac{\partial V}{\partial q_m} + \eta_1 \cdot \left(\frac{\partial f_1}{\partial q_m}\right) = 0, \tag{15}$$

are satisfied for every $m = 1,\ldots,6$. The coefficient η_1 is a Lagrange multiplier. Now, the system of Eqs. (12) and (13) can be written in compact matrix form as:

$$\mathbf{A}\cdot\mathbf{dq} = \mathbf{0}, \tag{16}$$

where the (2×6) matrix $\mathbf{A}$ is defined as:

$$\mathbf{A} = \left[\frac{\partial V}{\partial q_m} \quad \frac{\partial f_1}{\partial q_m}\right]^T, \tag{17}$$

and $\mathbf{dq}$ is the virtual generalized displacement vector:

$$\mathbf{dq} = [dq_1 \;\; dq_2 \;\; dq_3 \;\; dq_4 \;\; dq_5 \;\; dq_6]^T. \tag{18}$$

The kernel of $\mathbf{A}$ is of dimension: $(m_{\max} - p_{\max}) = (6-1) = 5$ (Lazopoulos and Markatis, 1994). Hence, Eq. (16) should be satisfied by five (5) independent solutions $\mathbf{dq}$. The space of these solutions is denoted by the matrix:

$$\mathbf{a} = [dq_{mr}], \quad m = 1,\ldots,6 \text{ and } r = 1,\ldots,5, \tag{19}$$

that satisfies the equation:

$$\mathbf{A}\cdot\mathbf{a} = \mathbf{0}. \tag{20}$$

It is noted that the space spanned by $\mathbf{a}$ is exactly the space of the generalized virtual vectors. Moreover, having defined vector $\mathbf{a}'$ and matrix $\mathbf{A}$, Eq. (15) is written again in compact form as:

$$\mathbf{a}'\cdot\mathbf{A} = \mathbf{0}. \tag{21}$$

Therefore, the equilibrium condition for the elastic system is expressed by the two reciprocal equations (20) and (21). The mappings $\mathbf{a}$ and $\mathbf{a}'$ are the kernel and co-kernel of $\mathbf{A}$, respectively, identifying linear mappings with their images (Porteous, 1971, 1994). Evidently, the values of the elements of $\mathbf{A}$ depend on the equilibrium point.

Studying further the equilibrium of the system in the generalized six-dimensional coordinate space q_m at the point q_m^0, under the action of the three-dimensional control parameters t_n^0, we denote by $\mathbf{y}(q_m; t_n)$ the nine-dimensional space of the generalized coordinates and control parameters. If we consider $\mathbf{y^0}(q_m^0; t_n^0)$ to be an equilibrium point, then the problem is now stated as: *Perturbing the parameters t_n^0, so that $t_n = t_n^0 + dt_n$ (with $|dt_n| \ll 1$), find the new equilibrium generalized displacement vector $q_m = q_m^0 + dq_m$ in the neighborhood of the equilibrium placement q_m^0.* It must be stressed that stable elastic systems are characterized by unique incremental displacement vectors dq_m; albeit, the critical states are distinguished by the existence of multiple incremental generalized displacement vectors. When, under the action of the incremental loading parameters dt_n, no dq_m can be found, equilibrium breaks down and dynamic response (motion) of the system is expected. Since the perturbed equilibrium placement $\mathbf{y}$ satisfies the equilibrium equation, the Taylor expansion of Eq. (20) around the primary equilibrium point $\mathbf{y^0}$ yields:

$$[\mathbf{A}\cdot\mathbf{a}]_{\mathbf{y}} = [\mathbf{A}\cdot\mathbf{a}]_{\mathbf{y^0}} + [\mathbf{B}\cdot\mathbf{a}]_{\mathbf{y^0}}\cdot\mathbf{dq} + [\mathbf{A}\cdot\mathbf{da}]_{\mathbf{y^0}} + [\mathbf{A_t}\cdot\mathbf{a}]_{\mathbf{y^0}}\cdot\mathbf{dt} + (\mathbf{h.o.t.}), \tag{22}$$

where

$$\mathbf{B} = \frac{\partial\mathbf{A}}{\partial\mathbf{q}} = \left[\left[\frac{\partial^2 V}{\partial q_r \partial q_s}\right] \quad \left[\frac{\partial^2 f_1}{\partial q_r \partial q_s}\right]\right]^{\mathbf{T}}, \quad r,s = 1,\ldots,6, \tag{23}$$

$$\mathbf{A_t}=\frac{\partial \mathbf{A}}{\partial \mathbf{t}}=\left[\begin{bmatrix}\frac{\partial^2 V}{\partial q_1\partial t_1} & \frac{\partial^2 V}{\partial q_1\partial t_2} & \frac{\partial^2 V}{\partial q_1\partial t_3}\\ \vdots & \vdots & \vdots\\ \frac{\partial^2 V}{\partial q_6\partial t_1} & \frac{\partial^2 V}{\partial q_6\partial t_2} & \frac{\partial^2 V}{\partial q_6\partial t_3}\end{bmatrix}\begin{bmatrix}\frac{\partial^2 f_1}{\partial q_1\partial t_1} & \frac{\partial^2 f_1}{\partial q_1\partial t_2} & \frac{\partial^2 f_1}{\partial q_1\partial t_3}\\ \vdots & \vdots & \vdots\\ \frac{\partial^2 f_1}{\partial q_6\partial t_1} & \frac{\partial^2 f_1}{\partial q_6\partial t_2} & \frac{\partial^2 f_1}{\partial q_6\partial t_3}\end{bmatrix}\right]^{\mathbf{T}}. \tag{24}$$

Dropping the subscript notation and recalling that both the initial $\mathbf{y^0}$ and the perturbed placement $\mathbf{y}$ satisfy Eq. (20), the governing equilibrium equation is simplified to:

$$\mathbf{B}\cdot\mathbf{a}\cdot\mathbf{dq}+\mathbf{A}\cdot\mathbf{da}=-\mathbf{A_t}\cdot\mathbf{a}\cdot\mathbf{dt}+(\mathbf{h.o.t.}), \tag{25}$$

keeping in mind that it refers to the primary equilibrium placement. The left-hand side (LHS) of equilibrium equation (25) is its linear part with respect to ($\mathbf{dq}$,$\mathbf{da}$), whereas the right-hand side (RHS) is the non-homogenous part, respectively. It is evident that a critical state has been reached when the L.H.S accepts a solution ($\mathbf{dq}$,$\mathbf{da}$) such that:

$$\mathbf{B}\cdot\mathbf{a}\cdot\mathbf{dq}+\mathbf{A}\cdot\mathbf{da}=0. \tag{26}$$

Let us consider an incremental vector $\mathbf{dq}$ satisfying equilibrium equation (16). As it was determined above, the vector $\mathbf{dq}$ lies in the (6×5) space defined by matrix $\mathbf{a}$. Therefore, $\mathbf{dq}$ is a one-dimensional vector in the five-dimensional space of $\mathbf{a}$. Consequently, there exists an injective linear map $\mathbf{a_1}:\mathbb{R}^1\to\mathbb{R}^5$ such that the image of the composition $(\mathbf{a}\cdot\mathbf{a_1})$ is the space generated by the vector $\mathbf{dq}$. Hence, Eq. (26) may be written in the following form:

$$\mathbf{B}\cdot\mathbf{a}\cdot(\mathbf{a}\cdot\mathbf{a_1})+\mathbf{A}\cdot\mathbf{da}=0. \tag{27}$$

Upon application of the co-kernel $\mathbf{a}'$ to the last expression and recalling equilibrium equation (21) emerges the relation:

$$\mathbf{L}[\mathbf{dq}]=\mathbf{L}[\mathbf{a}\cdot\mathbf{a_1}]=\mathbf{a}'\cdot\mathbf{B}\cdot\mathbf{a^2}\cdot\mathbf{a_1}=\mathbf{0}. \tag{28}$$

Furthermore, solving Eq. (27) for:

$$\mathbf{da}=-\mathbf{A^{-1}}\cdot(\mathbf{B}\cdot\mathbf{a}\cdot(\mathbf{a}\cdot\mathbf{a_1}))=\mathbf{b}\cdot\mathbf{a_1}, \tag{29}$$

it can now be stated again as:

$$(\mathbf{B}\cdot\mathbf{a}^2+\mathbf{A}\cdot\mathbf{b})\cdot\mathbf{a_1}=\mathbf{0}, \tag{30}$$

where $\mathbf{b}:\mathbb{R}^1\to L(\mathbb{R}^5,\mathbb{R}^6)$ is a symmetric bilinear map.

As it was demonstrated, the surface of critical points (Porteous, 1971, 1994), is defined by the system of Eqs. (20) and (30). The former is the equation describing the manifold of the equilibrium points in $(\mathbb{R}^6\times\mathbb{R}^3)$, whereas the latter is the critical condition describing the submanifold of critical points. Differentiating the system of Eqs. (20) and (30), the tangent space of the submanifold (surface) is described by:

$$\mathbf{B}\cdot\mathbf{a}\cdot\mathbf{dq}+\mathbf{A}\cdot\mathbf{da}+\mathbf{A_t}\cdot\mathbf{a}\cdot\mathbf{dt}=\mathbf{0}, \tag{31}$$

$$\begin{aligned}&(\mathbf{C}\cdot\mathbf{a^2}+\mathbf{B}\cdot\mathbf{b})\cdot\mathbf{dq}\cdot\mathbf{a_1}+\mathbf{B}\cdot(\mathbf{a}\cdot\mathbf{a_1})\cdot\mathbf{da}+\mathbf{B}\cdot\mathbf{da}\cdot(\mathbf{a_1}\cdot\mathbf{a})\\&+\mathbf{A}\cdot\mathbf{db}\cdot\mathbf{a_1}+(\mathbf{B}\cdot\mathbf{a^2}+\mathbf{A}\cdot\mathbf{b})\cdot\hat{\mathbf{a}}_1+(\mathbf{B_t}\cdot\mathbf{a^2}\cdot\mathbf{a_1}+\mathbf{A_t}\cdot\mathbf{b}\cdot\mathbf{a_1})\cdot\mathbf{dt}=\mathbf{0},\end{aligned} \tag{32}$$

where $\mathbf{C}=\partial\mathbf{B}/\partial\mathbf{q}$, $\hat{\mathbf{a}}_1=\mathbf{da_1}$, and:

$$\mathbf{B_t}=\frac{\partial\mathbf{B}}{\partial\mathbf{t}}=\begin{bmatrix}\left[\frac{\partial^3 V}{\partial q_r\partial q_s\partial t_1}\right] & \left[\frac{\partial^3 V}{\partial q_r\partial q_s\partial t_2}\right] & \left[\frac{\partial^3 V}{\partial q_r\partial q_s\partial t_3}\right]\\ \left[\frac{\partial^3 f_1}{\partial q_r\partial q_s\partial t_1}\right] & \left[\frac{\partial^3 f_1}{\partial q_r\partial q_s\partial t_2}\right] & \left[\frac{\partial^3 f_1}{\partial q_r\partial q_s\partial t_3}\right]\end{bmatrix},\quad r,s=1,\ldots,6. \tag{33}$$

It is pointed out that the set of the submanifold critical points is defined when there exists a vector $\mathbf{dq}$ lying in the kernel space of $\mathbf{L}$, Eq. (28), satisfying Eqs. (31) and (32) with $\mathbf{dt}=0$ (Lazopoulos and Markatis, 1994). Hence, the non-zero solution of the system:

$$\mathbf{B}\cdot\mathbf{a}\cdot\mathbf{dq}+\mathbf{A}\cdot\mathbf{da}=\mathbf{0}, \tag{34}$$

$$\begin{aligned}&(\mathbf{C}\cdot\mathbf{a^2}+\mathbf{B}\cdot\mathbf{b})\cdot\mathbf{dq}\cdot\mathbf{a_1}+\mathbf{B}\cdot(\mathbf{a}\cdot\mathbf{a_1})\cdot\mathbf{da}+\mathbf{B}\cdot\mathbf{da}\cdot(\mathbf{a_1}\cdot\mathbf{a})\\&+\mathbf{A}\cdot\mathbf{db}\cdot\mathbf{a_1}+(\mathbf{B}\cdot\mathbf{a^2}+\mathbf{A}\cdot\mathbf{b})\cdot\hat{\mathbf{a}}_1=\mathbf{0},\end{aligned} \tag{35}$$

defines the singular set of critical points. Recalling that $\mathbf{dq}=\mathbf{a}\cdot\mathbf{a_1}$ and applying the vector $\mathbf{a_1}$ and the co-kernel $\mathbf{a}'$ to Eq. (35), a more simplified form emerges:

$$\mathbf{a}'\cdot\mathbf{C}\cdot(\mathbf{a}\cdot\mathbf{a_1})^3+3\mathbf{a}'\cdot\mathbf{B}\cdot(\mathbf{a}\cdot\mathbf{a_1})\cdot(\mathbf{b}\cdot\mathbf{a_1^2})=0. \tag{36}$$

The critical points satisfying Eqs. (20) and (30) but failing to satisfy Eq. (36) are classified according to Thom's classification theorem as fold points (A_2) (Thom, 1975; Arnol'd, 1975). In addition, Eq. (35) may be equivalently written in the form:

$$\begin{aligned}&\mathbf{C}\cdot(\mathbf{a}\cdot\mathbf{a_1})^2\cdot\mathbf{a}+2\mathbf{B}\cdot(\mathbf{a}\cdot\mathbf{a_1})\cdot(\mathbf{b}\cdot\mathbf{a_1})+\mathbf{B}\cdot(\mathbf{b}\cdot\mathbf{a_1})^2\cdot\mathbf{a}\\&+\mathbf{A}\cdot\mathbf{c}\cdot\mathbf{a_1^2}+(\mathbf{B}\cdot\mathbf{a^2}+\mathbf{A}\cdot\mathbf{b})\cdot\hat{\mathbf{a}}_1=\mathbf{0},\end{aligned} \tag{37}$$

where $\mathbf{c}:\mathbb{R}\to L(\mathbb{R},L(\mathbb{R}^5,\mathbb{R}^6))$. Applying vector $\mathbf{a_1}$ to the last equation, this is simplified to:

$$\mathbf{C}\cdot(\mathbf{a}\cdot\mathbf{a_1})^3+3\mathbf{B}\cdot(\mathbf{a}\cdot\mathbf{a_1})\cdot(\mathbf{b}\cdot\mathbf{a_1^2})+\mathbf{A}\cdot\mathbf{c}\cdot\mathbf{a_1^3}=\mathbf{0}. \tag{38}$$

Thus, the multilinear matrix $\mathbf{c}$ is defined by Eq. (38). Considering the higher than the fold singularities surface, we proceed to the classification of the cusp singularities. To this end, that surface is defined by the system of Eqs. (20), (30) and (37), where the last equation is the cusp condition; all three equations describe the manifold of the cusp points (A_3) (Thom, 1975; Arnol'd, 1975). By following the same procedure, i.e., differentiating Eq. (37), the set of the cusp surface singular points is located when this tangent space ($\mathbf{dv}$,$\mathbf{dt}$) accepts a virtual vector ($\mathbf{dv}$,$\mathbf{0}$). Consequently, the singularity set higher than the cusp is defined by the system of Eqs. (20), (30) and (37) and:

$$\begin{aligned}\mathbf{a}'\Big\{&\mathbf{D}(\mathbf{a}\cdot\mathbf{a_1})^4+6\mathbf{C}\cdot(\mathbf{a}\cdot\mathbf{a_1})^2\cdot(\mathbf{b}\cdot\mathbf{a_1^2})+\mathbf{B}\cdot(\mathbf{c}\cdot\mathbf{a_1^3})\cdot(\mathbf{a}\cdot\mathbf{a_1})\\&+2\mathbf{C}\cdot(\mathbf{a}\cdot\mathbf{a_1})^2\cdot(\mathbf{a}\cdot\hat{\mathbf{a}}_1)+2\mathbf{B}\cdot\Big[(\mathbf{b}\cdot\mathbf{a_1^2})^2+(\mathbf{b}\cdot\mathbf{a_1^2})\cdot(\mathbf{b}\cdot\mathbf{a_1}\cdot\hat{\mathbf{a}}_1)\\&+(\mathbf{a}\cdot\mathbf{a_1})(\mathbf{c}\cdot\mathbf{a_1^3}+\mathbf{b}\cdot\mathbf{a_1}\cdot\hat{\mathbf{a}}_1)\Big]+\mathbf{C}\cdot(\mathbf{a}\cdot\hat{\mathbf{a}}_1)\cdot(\mathbf{a}\cdot\mathbf{a_1})^2\\&+\mathbf{B}\cdot(\mathbf{a}\cdot\hat{\mathbf{a}}_1)\cdot(\mathbf{b}\cdot\mathbf{a_1^2})+\mathbf{B}\cdot(\mathbf{b}\cdot\mathbf{a_1}\cdot\hat{\mathbf{a}}_1)\cdot(\mathbf{a}\cdot\mathbf{a_1})\\&+\mathbf{B}\cdot(\mathbf{a}\cdot\mathbf{a_1})\cdot(\mathbf{b}\cdot\mathbf{a_1}\cdot\hat{\mathbf{a}}_1)\Big\}=0,\end{aligned} \tag{39}$$

where $\mathbf{D}=\partial\mathbf{C}/\partial\mathbf{q}$. Since in this work only the simple singularities will be considered, the reader is referred to the literature (Lazopoulos and Markatis, 1994; Lazopoulos, 2006), for explicit formulae concerning the higher singularities. In any case, the procedure followed is the one that is outlined in the present paragraph.

Applying the co-kernel $\mathbf{a}'$ directly to Eq. (25) and taking into account Eq. (21), the equilibrium equation is written again as:

$$\mathbf{a}'\cdot\mathbf{B}\cdot\mathbf{a^2}\cdot\mathbf{a_1}=-\mathbf{a}'\cdot\mathbf{A}_t\cdot\mathbf{a}\cdot\mathbf{dt}+(\mathbf{h.o.t.}). \tag{40}$$

Eq. (40) defines the unknown mapping $\mathbf{a_1}$ uniquely if no solution exists such that satisfies the linear homogeneous equation (28). In this case, Eq. (40) yields:

$$\mathbf{a_1}=(\mathbf{a}'\cdot\mathbf{B}\cdot\mathbf{a^2})^{-1}\cdot(-\mathbf{a}'\cdot\mathbf{A}_t\cdot\mathbf{a}\cdot\mathbf{dt})+(\mathbf{h.o.t.}), \tag{41}$$

which is the unique solution to the equilibrium problem. Nevertheless, when a non-zero solution $\mathbf{a_1}$ satisfying Eq. (28) exists, bifurcation of the equilibrium path takes place. When the dimension of the kernel space is equal to one the bifurcation is called *simple*, whereas for higher than one-dimensional kernel the bifurcation is called*compound*.

According to formal branching theory (Vainberg and Trenogin, 1974), for the simple or one-dimensional branching, the equilibrium path is defined by:

$$\mathbf{dq}=\xi\cdot(\mathbf{a}\cdot\mathbf{a_1})+\mathbf{o}(\xi). \tag{42}$$

Since $(\mathbf{a}\cdot\mathbf{a_1})$ represents the kernel space in the six-dimensional space of $\mathbf{q}$; ξ is a small parameter to be defined by the higher order terms of the Taylor expansion, Eq. (25), as a function of the

incremental loading parameters **dt**. Proceeding to the evaluation of the parameter ξ one gets (Lazopoulos, 1994):

$$\xi^2 = -\frac{2\mathbf{a}'\cdot\mathbf{A_t}\cdot\mathbf{a}\cdot\mathbf{a_1}\cdot\mathbf{dt}}{\mathbf{a}'\cdot\mathbf{C}\cdot(\mathbf{a}\cdot\mathbf{a_1})^3+3\mathbf{a}'\cdot\mathbf{B}\cdot(\mathbf{a}\cdot\mathbf{a_1})\cdot(\mathbf{b}\cdot\mathbf{a_1})^2}. \tag{43}$$

Eq. (43) is valid only when the denominator has a different than zero value and the RHS is positive; in the case of a negative signed RHS equilibrium breaks down. As it was mentioned in the previous section, the present singularity is classified as fold and in the case that the aforementioned denominator is equal to zero, higher order terms of the Taylor expansion should be considered as higher singularities emerge.

4. The compound branching problem

When the space $\mathbf{a_1}$ of the solutions to Eq. (28) is of dimension two, compound bifurcation has been located where the interaction of instability modes takes place. In this case, there exist two independent solutions $\boldsymbol{\phi_1}$ and $\boldsymbol{\phi_2}$ of the aforesaid linear homogeneous equation. If we call $\boldsymbol{\delta}$ this kernel then:

$$\boldsymbol{\delta} = [\boldsymbol{\phi_1}\ \ \boldsymbol{\phi_2}]. \tag{44}$$

Moreover, any vector in the space $\boldsymbol{\delta}$ is defined by the linear combination of the vectors $\boldsymbol{\phi_1}$ and $\boldsymbol{\phi_2}$, hence:

$$\mathbf{a_1} = \xi_1\cdot\boldsymbol{\phi_1} + \xi_2\cdot\boldsymbol{\phi_2} = \boldsymbol{\delta}\cdot\boldsymbol{\gamma}, \tag{45}$$

where

$$\boldsymbol{\gamma} = [\xi_1\ \ \xi_2]^{\mathbf{T}}. \tag{46}$$

The necessary condition for the existence of compound branching is expressed as

$$\mathbf{a}'\cdot\mathbf{B}\cdot\mathbf{a^2}\cdot\boldsymbol{\delta} = 0. \tag{47}$$

Furthermore, the branching equation (47) is equivalent to:

$$(\mathbf{B}\cdot\mathbf{a}^2+\mathbf{A}\cdot\mathbf{b})\cdot\boldsymbol{\delta} = \mathbf{0}. \tag{48}$$

The equivalent relations (47) and (48) depend on the linear terms of the elastic system and yield the critical conditions for compound bifurcation along with the instability modes $\mathbf{a}\cdot\boldsymbol{\phi_1}$, $\mathbf{a}\cdot\boldsymbol{\phi_2}$.

The definition of the post-critical equilibrium paths in the compound bifurcation case is a complicated problem even for unconstrained systems due to interaction of the instability modes. As it was briefly mentioned in the introduction, standard mathematical procedures require elimination of the passive coordinates and normalization of the energy function; more advanced methods lift these requirements, yet the problem is not simple and needs elaborate mathematical treatment. The tangent vector to the equilibrium path at the critical point lies in the space of the kernel of the linear homogeneous problem. Considering the definition of a critical curve, this is described by the simultaneous solution of the equilibrium and branching equations. Indeed, the loading parameters can be adjusted in order that every point of a curve is critical with one-dimensional kernel that varies from point to point in the neighborhood of a compound branching point. Once again, the critical equilibrium paths are defined by the equations:

$$(\mathbf{a}'\cdot\mathbf{A})|_{\mathbf{y}} = \mathbf{0} \quad \text{or} \quad (\mathbf{A}\cdot\mathbf{a})|_{\mathbf{y}} = \mathbf{0}, \tag{49}$$

$$(\mathbf{B}\cdot\mathbf{a}^2+\mathbf{A}\cdot\mathbf{b})|_{\mathbf{y}}\cdot\mathbf{a_1}(\mathbf{y}) = \mathbf{0} \quad \text{or} \quad (\mathbf{a}'\cdot\mathbf{B}\cdot\mathbf{a^2})|_{\mathbf{y}}\cdot\mathbf{a_1}(\mathbf{y}) = \mathbf{0}, \tag{50}$$

where $\mathbf{a_1}(\mathbf{y})$ represents the one-dimensional variable kernel of the linear homogeneous equation (50). It is evident that these critical curves pass through the compound critical point (Lazopoulos, 1994). Any equilibrium path including a bifurcation point is tangent to the critical curve and their common tangent lies in the kernel $\mathbf{a_1}(q_i,t_j)$.

In order to define the tangent vector to the critical curves, differentiation of Eqs. (49a) and (50a) yields:

$$[\mathbf{B}\cdot\mathbf{a}\cdot\mathbf{dq}+\mathbf{A}\cdot\mathbf{da}+\mathbf{A_t}\cdot\mathbf{a}\cdot\mathbf{dt}]|_{\mathbf{y}} = \mathbf{0}, \tag{51}$$

$$\begin{aligned}&[(\mathbf{C}\cdot\mathbf{a}^2+\mathbf{B}\cdot\mathbf{b})\cdot\mathbf{a_1}\cdot\mathbf{dq}+(\mathbf{B_t}\cdot\mathbf{a^2}+\mathbf{A_t}\cdot\mathbf{b})\cdot\mathbf{a_1}\cdot\mathbf{dt}\\&+(2\mathbf{B}\cdot\mathbf{a}\cdot\mathbf{da}+\mathbf{A}\cdot\mathbf{db})\cdot\mathbf{a_1}+(\mathbf{B}\cdot\mathbf{a^2}+\mathbf{A}\cdot\mathbf{b})\cdot\mathbf{db}]|_{\mathbf{y}} = \mathbf{0}.\end{aligned} \tag{52}$$

Now that a critical curve has been considered, all its points are branching points and its tangent vector lies in the kernel corresponding at that point. Further, substituting the appropriate expressions for **dq** and **da** as outlined in Section 3 and upon application of the co-kernel $\mathbf{a}'$, Eq. (52) is simplified to:

$$\begin{aligned}&[\mathbf{a}'\cdot(\mathbf{C}\cdot\mathbf{a}^2+\mathbf{B}\cdot\mathbf{b})\cdot\mathbf{a_1}\cdot\mathbf{a}\cdot\mathbf{a_1}+\mathbf{a}'\cdot(\mathbf{B_t}\cdot\mathbf{a^2}+\mathbf{A_t}\cdot\mathbf{b})\cdot\mathbf{a_1}\cdot\mathbf{dt}\\&+\mathbf{a}'\cdot(2\mathbf{B}\cdot\mathbf{a}\cdot\mathbf{b}\cdot\mathbf{a_1})\cdot\mathbf{a_1}]|_{\mathbf{y}} = \mathbf{0}.\end{aligned} \tag{53}$$

When the point **y** of the critical curve reaches the compound critical point $\mathbf{y}^0$, the tangent vector $\mathbf{a_1}$ lies in the two-dimensional kernel $\boldsymbol{\delta}$ and is defined at this equilibrium placement of compound bifurcation by Eq. (45). Consequently, as the critical point, tracing the critical curve, reaches the compound bifurcation point, Eq. (53) becomes:

$$\begin{aligned}&\mathbf{a}'\cdot(\mathbf{C}\cdot\mathbf{a}^2+\mathbf{B}\cdot\mathbf{b})\cdot\mathbf{a}\cdot(\boldsymbol{\delta}\cdot\boldsymbol{\gamma})^2+\mathbf{a}'\cdot(\mathbf{B_t}\cdot\mathbf{a^2}+\mathbf{A_t}\cdot\mathbf{b})\cdot(\boldsymbol{\delta}\cdot\boldsymbol{\gamma})\cdot\mathbf{dt}\\&+2\mathbf{a}'\cdot\mathbf{B}\cdot\mathbf{a}\cdot\mathbf{b}\cdot(\boldsymbol{\delta}\cdot\boldsymbol{\gamma})^2 = \mathbf{0}.\end{aligned} \tag{54}$$

This last expression yields the vectors $\boldsymbol{\gamma}$ with respect to the incremental loading **dt**. Nevertheless, a more convenient way for the definition of $\boldsymbol{\gamma}$ is revealed when Eq. (54) is multiplied by an auxiliary vector $(\boldsymbol{\delta}\cdot\mathbf{n})$, normal to $(\boldsymbol{\delta}\cdot\boldsymbol{\gamma})$ in the sense that:

$$\mathbf{a}'\cdot(\mathbf{B_t}\cdot\mathbf{a^2}+\mathbf{A_t}\cdot\mathbf{b})\cdot(\boldsymbol{\delta}\cdot\boldsymbol{\gamma})\cdot(\boldsymbol{\delta}\cdot\mathbf{n})\cdot\mathbf{dt} = 0. \tag{55}$$

Accordingly, applying vector $(\boldsymbol{\delta}\cdot\mathbf{n})$ to Eq. (54) yields:

$$\begin{aligned}&\mathbf{a}'\cdot\mathbf{C}\cdot\mathbf{a}^2\cdot(\boldsymbol{\delta}\cdot\boldsymbol{\gamma})^2\cdot(\mathbf{a}\cdot(\boldsymbol{\delta}\cdot\mathbf{n}))+\mathbf{a}'\cdot\mathbf{B}\cdot\mathbf{b}\cdot(\mathbf{a}\cdot(\boldsymbol{\delta}\cdot\mathbf{n}))\cdot(\boldsymbol{\delta}\cdot\boldsymbol{\gamma})^2\\&+2\mathbf{a}'\cdot\mathbf{B}\cdot(\mathbf{a}\cdot(\boldsymbol{\delta}\cdot\mathbf{n}))\cdot\mathbf{b}\cdot(\boldsymbol{\delta}\cdot\boldsymbol{\gamma})\cdot(\boldsymbol{\delta}\cdot\mathbf{n}) = 0.\end{aligned} \tag{56}$$

Algebraic equations (55) and (56) comprise a system whose solutions with respect to the vector $\boldsymbol{\gamma}$ define the tangent directions to the equilibrium paths. Furthermore, the number of these solutions classifies the umbilic singularity: one solution-vector $\boldsymbol{\gamma}$ corresponds to hyperbolic umbilic (D_4^+), whereas two to parabolic (D_5), and three to an elliptic umbilic singularity (D_4^-) (Arnol'd, 1975).

5. Applications

In the preceding sections, a detailed free coordinate bifurcation analysis of the constrained tensegrity model was provided for the detection and classification of the various singularities, as well as the description of post-equilibrium paths. In this section, theory is implemented by two applications focusing on the effects of the instability modes. The structure loses stability either due to Euler buckling of the bars (local instability), or as a result of the behaviour of the overall system (global instability). However, it may also occur that the two instability modes interact and then compound bifurcation emerges. In the general non-compound case, depending on the various geometrical, material and loading parameters, the local instability may precede the global, or appear after it.

The presented study of the system in hand was performed under the application of a general triaxial loading. Henceforth, it is assumed that the external loading is equitriaxial (hydrostatic-like). The current system under this type of symmetric loading is similar to the case of Rivlin's cube. It is recalled that when a cube of incompressible material is subjected to equitriaxial loading, it is deformed in such a way that it evolves into a rectangular

parallelepiped occupying the same volume as the original cube (Rivlin, 1948, 1974; Ogden, 1997; Golubitsky et al., 1988).

Before we proceed to any numerical investigation of the model, it is instructive to examine further the necessary conditions for branching of its equilibrium that present a more complex behaviour than was initially expected. It is reminded that critical points are located as solutions to the system of Eqs. (20), (21) and (28), or its counterpart equation (30), under the influence of the constraint of Eq. (10). Moreover, in the case of instability mode interaction the kernel $\boldsymbol{\delta}$ is of codimension two, which according to what is known from Algebra indicates that *all minor determinants of matrix* $(\mathbf{a}' \cdot \mathbf{B} \cdot \mathbf{a}^2)$ *should be equal to zero*; this secures the emergence of compound bifurcation. For the system under consideration, it is revealed that for any suitable choice of linearly independent generalized virtual vectors **dq** comprising matrix **a** and simultaneously satisfying the aforementioned equations, e.g.:

$$\mathbf{a} = \begin{bmatrix} 1 & 0 & 0 & 0 & 0 \\ -1 & 1 & 0 & 0 & 0 \\ 0 & -1 & 0 & 0 & 0 \\ 0 & 0 & 1 & 0 & 0 \\ 0 & 0 & 0 & 1 & 0 \\ 0 & 0 & 0 & 0 & 1 \end{bmatrix}, \tag{57}$$

when used in order to construct the critical condition for branching:

$$\det(\mathbf{a}' \cdot \mathbf{B} \cdot \mathbf{a}^2) = 0, \tag{58}$$

produce matrices of the form:

$$\begin{bmatrix} 2h & -h & 0 & 0 & 0 \\ -h & 2h & 0 & 0 & 0 \\ 0 & 0 & 0 & 0 & 0 \\ 0 & 0 & 0 & 0 & 0 \\ 0 & 0 & 0 & 0 & 0 \end{bmatrix} = 0. \tag{59}$$

It is evident that the value of the (2×2) minor:

$$\det \begin{bmatrix} 2h & -h \\ -h & 2h \end{bmatrix} = 3h^2, \tag{60}$$

is equal to zero only if $h = 0$. This, taken into account along with the correspondence of the dq_i in Eq. (57), suggests that the global instability mode accepts a two-dimensional kernel, and consequently, for the interaction of instability modes a three-dimensional kernel should be employed. In the following we provide specific examples of how to treat the two distinct instability modes, whereas for a three-dimensional kernel (interaction) the mathematical apparatus demands further elaboration and the interested reader is referred to the literature (Pignataro and Luongo, 1994).

5.1. One-dimensional branching

In this paragraph, the case of one-dimensional branching due to local Euler buckling of the bars is presented. To this end, we consider the structure of Fig. 1 with compression-bearing elements that are allowed to buckle and geometric, material and loading parameters relevant to CSK mechanics. Since bars are supposed to correspond to microtubules and strings to the actin filament network we assign the physiologically typical values $L_0 = 3\ \mu\text{m}$ and $l_0 = 1\ \mu\text{m}$ for the inextensible curve of the bars and rest length of the strings, respectively (Stamenović, 2008). Furthermore, the bending stiffness of the bars is assumed to be $k_B = 26\ \text{pN}\ \mu\text{m}^2$ (Kamm and Mofrad, 2006), while the elastic moduli of the strings are considered as: $k_1 = 0.1005\ \text{pN}\ \mu\text{m}$, $k_2 = 30.7008\ \text{pN}\ \mu\text{m}$, and $k_3 = -4.38489\ \text{pN}\ \mu\text{m}$. For these values and $c = 3.375\ \mu\text{m}^3$, the set of Eqs. (10), (20), (21) and (58) is solved simultaneously and produces the critical equilibrium point: $(s_X = s_Y = s_Z = 1.5\ \mu\text{m},\ \zeta_1 = \zeta_2 = \zeta_3 = 0;\ T_X = T_Y = T_Z = -5.44686\ \text{pN})$ with $\eta_1 = -2.42083$. It is reminded that Eqs. (21) express force equilibrium for the system under the constraint of Eqs. (10) and (20) are the reciprocal equations to Eqs. (21) and (58) is the necessary condition for branching of the equilibrium.

The fact that the symmetric configuration represented by these parameter values is critical for buckling can be independently verified by simple analysis of force equilibrium at the end of the bars. At this particular equilibrium point, the critical conditions for buckling hold identically, i.e.:

$$\frac{\partial^2 \widetilde{V}}{\partial \zeta_1^2} = \frac{\partial^2 \widetilde{V}}{\partial \zeta_2^2} = \frac{\partial^2 \widetilde{V}}{\partial \zeta_3^2} = 0, \tag{61}$$

where $\widetilde{V} = V + \eta_1 \cdot f_1$. Simple algebra reveals that Eqs. (61) are equivalent to the equations (Coughlin and Stamenović, 1997):

$$F_1 \frac{L_1}{l_1} + F_2 \frac{L_1 - s_Z}{l_2} = k_B \left(\frac{\pi}{L_0}\right)^2, \tag{62}$$

$$F_3 \frac{L_2}{l_3} + F_1 \frac{L_2 - s_X}{l_1} = k_B \left(\frac{\pi}{L_0}\right)^2, \tag{63}$$

$$F_2 \frac{L_3}{l_2} + F_3 \frac{L_3 - s_Y}{l_3} = k_B \left(\frac{\pi}{L_0}\right)^2, \tag{64}$$

where F_1, F_2, F_3 denote tensile forces in strings with lengths l_1, l_2, l_3, respectively. Eqs. (62)–(64) are static equilibrium equations of the model and their RHS represents the axial compressive force exerted on each bar. It is straightforward that in this case the compressive force is equal to the Euler critical load for buckling.

At the critical configuration, matrix **A** is expressed as

$$\mathbf{A} = \begin{bmatrix} 5.44686 & 5.44686 & 5.44686 \\ 2.25 & 2.25 & 2.25 \end{bmatrix}, \tag{65}$$

with the space **a** defined by Eq. (57). Further, at the point we are discussing the matrix $(\mathbf{a}' \cdot \mathbf{B} \cdot \mathbf{a}^2)$ accepts a one-dimensional kernel:

$$\mathbf{a_1} = [0\ \ 0\ \ 1\ \ 1\ \ 1]^{\mathbf{T}}. \tag{66}$$

Consequently:

$$\mathbf{dq} = \mathbf{a} \cdot \mathbf{a_1} = [0\ \ 0\ \ 0\ \ 1\ 1\ \ 1]^T. \tag{67}$$

Proceeding to the classification of the singularity, the various matrixes are evaluated at the critical equilibrium point and the cusp condition – i.e., the LHS of Eq. (36) – yields:

$$\mathbf{a}' \cdot \mathbf{C} \cdot (\mathbf{a} \cdot \mathbf{a_1})^3 + 3\mathbf{a}' \cdot \mathbf{B} \cdot (\mathbf{a} \cdot \mathbf{a_1}) \cdot (\mathbf{b} \cdot \mathbf{a_1^2}) = 0. \tag{68}$$

Next, in order to investigate whether the singularity is higher than the cusp we calculate the LHS of Eq. (39), which for convenience we call Φ. The evaluation results to:

$$\Phi = 32497. \tag{69}$$

Therefore, the catastrophe is classified as cusp, (A_3), according to Thom's classification theorem (Thom, 1975; Arnol'd, 1975).

The total potential energy function in the neighborhood of the cusp singularity can be expressed as (Gilmore, 1981):

$$\begin{aligned} \widetilde{V} &= V + \eta_1 \cdot f_1 \\ &= \frac{\Phi}{4!} \cdot \xi^4 + \frac{1}{2} \cdot \xi^2 \cdot \left(\left.\frac{\partial^3 \widetilde{V}}{\partial q_i \partial q_j \partial t_a}\right|_{q_m^0} dq_i dq_j dt_a + \left.\frac{\partial^3 \widetilde{V}}{\partial q_i \partial q_j \partial t_b}\right|_{q_m^0} dq_i dq_j d\mu_b \right) \\ &\quad + \xi \cdot \left(\left.\frac{\partial^2 \widetilde{V}}{\partial q_i \partial t_a}\right|_{q_m^0} dq_i dt_a + \left.\frac{\partial^2 \widetilde{V}}{\partial q_i \partial t_b}\right|_{q_m^0} dq_i d\mu_b \right). \end{aligned} \tag{70}$$

Variables t_a and μ_b are general control parameters of the system, which here we consider to be the loading parameters T_X, T_Y, T_Z,

and rest length l_0, respectively. Now, if these control parameters are perturbed, i.e., $t_a = t_a^0 + dt_a$ and $\mu_b = l_0 + dl_0$ with $|dt_a|, |dl_0| \ll 1$, the potential energy function of the problem becomes:

$$\widetilde{V} = \frac{32497}{4!}\cdot\xi^4 + \frac{1}{2}\cdot\xi^2\cdot 2075\cdot dl_0. \tag{71}$$

Hence, the equilibrium equation yields:

$$\xi = 0, \quad \xi = \pm 0.618961\cdot\sqrt{-dl_0}. \tag{72}$$

Upon examination of Eq. (71) it is noticed that the coefficients corresponding to the loading increments (dT_X, dT_Y, dT_Z) vanish. This observation is in contrast to the case of the unconstrained system and it can be attributed to the effect of the constraint. Further, from Eq. (72) it is evident that the zero solution for ξ corresponds to the trivial case, whereas for the other two solutions special attention must be paid in the sign of the quantity under the square root. Up to this point of the analysis prestress has not been treated explicitly; albeit, it can be considered to be embedded in the terms $(l_j/l_0 - 1)$ and thus controlled by the value of the rest length. Hence, changing the rest length implies that, indirectly, the prestress is also changed. Since the effect of the loading increments is eliminated by the constrained, the axial compressive force at the end of the bars depends on the pulling forces exerted by the strings. Apparently, if all other parameters are kept constant, the pulling forces increase – and cause buckling – when the rest length is decreased. Therefore, the perturbation introduced to the rest length should be negative, i.e., $dl_0 < 0$. This certifies that the quantity under the square root in Eq. (72) is positive and provides a physical meaning for the appearance of the negative sign. Now, the post-buckling equilibrium paths are determined as follows:

$$\begin{bmatrix}\zeta_1\\ \zeta_2\\ \zeta_3\end{bmatrix} = \begin{bmatrix}0\\ 0\\ 0\end{bmatrix} \pm 0.618961\cdot\sqrt{-dl_0}\cdot\begin{bmatrix}1\\ 1\\ 1\end{bmatrix}. \tag{73}$$

It is evident that buckling of the bars causes a small decrease in the distance between their ends. In turn, this decrease suggests that the distances between the parallel bars are changed contrary to the assumption of the incompressibility constraint and Eq. (67). Nevertheless, this small change is of higher order of magnitude and may be neglected.

It is worth mentioning that this typical behaviour for the tensegrity model is also observable in living cells. Following contraction (increase in prestress) of the actin filament network by means of biochemical agents, microtubules that initially appeared straight in the relaxed state, now appear buckled (Wang et al., 2001).

5.2. Two-dimensional branching

In the following, we investigate the global instability mode of the tensegrity model of Fig. 1; however, it is now assumed that all the bars of the system are rigid. In this case, and in accordance to what was mentioned in the beginning of this section, branching of the equilibrium is two-dimensional. The analysis reveals that after the critical value of the external equitriaxial loading the structure loses symmetry in the way Rivlin's cube evolves into a rectangular parallelepiped and the corresponding post-equilibrium paths will be thoroughly described.

Upon considering the constrained tensegrity model with rigid bars, the number of free coordinates is now reduced to three (s_X, s_Y, s_Z), instead of six in the general case. Hence, the total potential energy function of the structure is rewritten in the proper compact form

$$V = V(q_m; t_n), \quad m = 1,2,3 \text{ and } n = 1,2,3. \tag{74}$$

The general analysis exposed in Sections 3 and 4 holds as is, with a corresponding reduce in matrix and mapping space dimensions.

To this end, we consider a tensegrity CSK model, under the constraint of Eq. (10), with the geometrical and material characteristics: $L_0 = 5\ \mu m$, $l_0 = 2\ \mu m$, $k_1 = 0.169646$ pN μm, $k_2 = 5.5488$ pN μm, $k_3 = -0.913319$ pN μm. For $c = 15.625\ \mu m^3$, Eqs. (10), (20), (21) and (58) provide the critical equilibrium point:

$$(s_X = s_Y = s_Z = 2.5\ \mu m;\ T_X = T_Y = T_Z = 2.78108\ \text{pN})$$

with $\eta_1 = 0.444973$. At this configuration, matrix **A** is expressed as

$$\mathbf{A} = \begin{bmatrix}-2.78108 & -2.78108 & -2.78108\\ 6.25 & 6.25 & 6.25\end{bmatrix}, \tag{75}$$

with the space **a** defined by

$$\mathbf{a} = \begin{bmatrix}1 & -2\\ 1 & 1\\ -2 & 1\end{bmatrix}. \tag{76}$$

The branching condition yields

$$\mathbf{a}'\cdot\mathbf{B}\cdot\mathbf{a}^2 = \begin{bmatrix}0 & 0\\ 0 & 0\end{bmatrix}, \tag{77}$$

wherefrom it is evident that a two-dimensional kernel should be employed. Such an appropriate one is:

$$\boldsymbol{\delta} = \begin{bmatrix}1 & 0\\ 0 & 1\end{bmatrix}. \tag{78}$$

Further, the implementation of Eqs. (55) and (56) is required for the definition of the tangents to the branching paths. To this end, we call:

$$\mu = \frac{\xi_1}{\xi_2} \quad \text{and} \quad \sigma = \frac{n_1}{n_2}, \tag{79}$$

and replace these ratios in the two equations. Next, we solve Eq. (55) for σ and replace it in Eq. (56); the result yields a cubic equation in μ:

$$\begin{aligned}&(-6.29107dT_X + 4.49362dT_Y)\cdot\mu^3 + (-2.16788dT_X\\ &\quad - 1.54848dT_Y + 5.39235dT_Z)\cdot\mu^2 + (3.71693dT_X\\ &\quad + 2.65495dT_Y + 1.85818dT_Z)\cdot\mu - 3.18594dT_Z = 0.\end{aligned} \tag{80}$$

It is evident that further investigation of the cubic equation is possible for various values of the loading increments ratios. In fact, there exist different values of these ratios for which Eq. (80) accepts three, two or one real solution. Thus, recalling that the applied external loading is equtriaxial, we assume that $dT_X = dT_Y = dT_Z$. Hence, Eq. (80) is now reduced to

$$-1.79745\mu^3 + 1.67599\mu^2 + 8.23006\mu - 3.18594 = 0, \tag{81}$$

which accepts the three solutions: $\mu_1 = -1.9248$, $\mu_2 = 0.370277$, $\mu_3 = 2.48695$, yielding the three tangent vectors:

$$\zeta_1\begin{bmatrix}-3.9248\\ -0.924804\\ 4.84961\end{bmatrix}, \quad \zeta_2\begin{bmatrix}-1.62972\\ 1.37028\\ 0.259445\end{bmatrix}, \quad \zeta_3\begin{bmatrix}0.486953\\ 3.48695\\ -3.97391\end{bmatrix}. \tag{82}$$

Therefore, the singularity is classified as elliptic umbilic (D_4^-) (Thom, 1975; Arnol'd, 1975). Now that the directions of the tangent vectors to the equilibrium paths have been defined, the analysis may continue further to describe the first order post-critical paths by evaluating the parameters ζ_i. Thus, substituting the results (82) in Eq. (54), one gets,

$$\begin{aligned}\zeta_1 &= -0.0448669dT_X - 0.0320478dT_Y + 0.0171125dT_Z,\\ \zeta_2 &= 0.0773882dT_X + 0.0552773dT_Y - 0.0295163dT_Z,\\ \zeta_3 &= 0.0231706dT_X + 0.0165504dT_Y - 0.00883739dT_Z.\end{aligned} \tag{83}$$

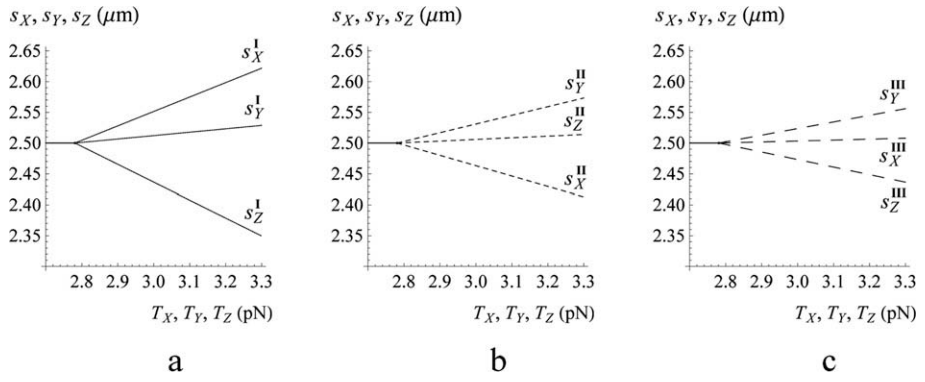

Fig. 2. The three post-critical equilibrium paths of Eq. (84) corresponding to: (a) q_m^{I}, (b) q_m^{II}, and (c) q_m^{III}.

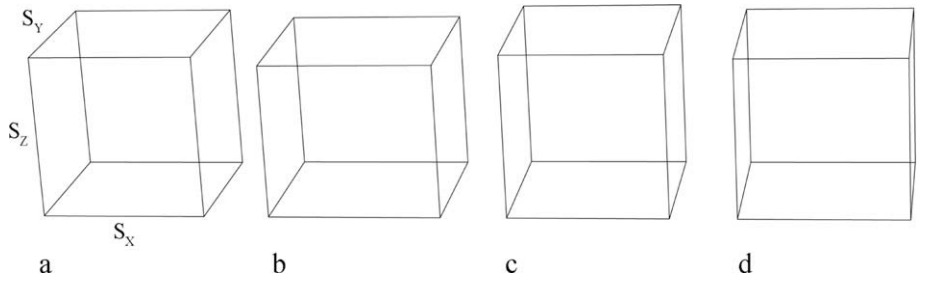

Fig. 3. Loss of symmetry past the critical loading (analogy to Rivlin's cube). The edges of the cube in (a) correspond to the distances between the pairs of parallel bars of the tensegrity model. Configuration (a) represents the symmetric pre-critical state ($s_X = s_Y = s_Z = 2.5$ μm). The rectangular parallelepipeds of (b), (c) and (d) have been constructed in the same fashion as the cube, after substituting the value $dT_X = dT_Y = dT_Z = 0.5$ pN in q_m^{I}, q_m^{II}, q_m^{III} (Eq. (84)), respectively.

Hence, the three post-critical equilibrium paths are described by the relations:

$$
\begin{aligned}
q_m^{\mathrm{I}} &= \begin{bmatrix} 2.5 \\ 2.5 \\ 2.5 \end{bmatrix} + (-0.0448669dT_X - 0.0320478dT_Y + 0.0171125dT_Z) \begin{bmatrix} -3.9248 \\ -0.924804 \\ 4.84961 \end{bmatrix}, \\
q_m^{\mathrm{II}} &= \begin{bmatrix} 2.5 \\ 2.5 \\ 2.5 \end{bmatrix} + (0.0773882dT_X + 0.0552773dT_Y - 0.0295163dT_Z) \begin{bmatrix} -1.62972 \\ 1.37028 \\ 0.259445 \end{bmatrix}, \\
q_m^{\mathrm{III}} &= \begin{bmatrix} 2.5 \\ 2.5 \\ 2.5 \end{bmatrix} + (0.0231706dT_X + 0.0165504dT_Y - 0.00883739dT_Z) \begin{bmatrix} 0.486953 \\ 3.48695 \\ -3.97391 \end{bmatrix},
\end{aligned}
\tag{84}
$$

and they are graphically illustrated in Fig. 2. As already mentioned in the beginning of the current paragraph and is evident from Fig. 2, the structure is symmetric and undeformed until the external loading reaches its critical value; symmetry here is mathematically translated to $s_X = s_Y = s_Z$ and $l_1 = l_2 = l_3$. Any further absolute increase of the loading increments results to loss of symmetry, as described by Eq. (84), such that the distances between the pairs of bars, and consequently the string lengths, become different with respect to each other (Fig. 3).

6. Discussion and conclusion

In this work, the singularities of a constrained tensegrity model were discussed. Critical conditions for branching of the equilibrium and classification of the emerging singularities has been performed. Further, a complete study of the mechanical response of the system produced explicit formulae for the definition of the post-critical equilibrium paths, yielding non-symmetric post-critical configurations of the tensegrity model.

The unconstrained version of the model under study has been extensively used in the past by several authors as a simplified case-study to investigate the application of the principles of tensegrity architecture in cytoskeletal mechanics. In this work, this characteristic CSK model was extended by introducing a geometrical constraint that is compatible to cell physiology, i.e., the observation that cells are incompressible. When the strings and bars of the model were identified as actin filaments and microtubules, respectively, and physiologically feasible geometric and material properties values were attributed to them, the forces and deformations resulting from the analysis were of the same order of magnitude as those observed in living cells, i.e., forces of the order of pN produce deformations of the order of μm (Coughlin and Stamenović, 1997; Boal, 2002). Further, although the model is an obvious oversimplification of CSK architecture, it is capable of reproducing such mechanical behaviours as the buckling of microtubules in response to cell contraction. This agreement between the model and mechanical behaviour of the CSK suggests that tensegrity may integrate fundamental mechanisms that control cellular mechanics.

The analysis also revealed important differences between the constrained and the unconstrained system. In contrast to the behaviour of the unconstrained system which is deformed under the action of any external loading, the incompressible system remains undeformed from the unloaded state until the critical conditions are met (Fig. 2). Moreover, in the case of the global instability of the unconstrained system branching is one-dimensional (Lazopoulos, 2005b), whereas for the incompressible system branching is compound. As a consequence, in order to study the interaction of instability modes of the constrained system a three-dimensional kernel should be considered, rather than the two-dimensional for the unconstrained. These differences can be clearly ascribed to the effect of the constraint. Although the studied tensegrity model is simple and presents three-dimensional sym-

metry, it also exhibits a rich mechanical response. It is evident that force equilibrium equations alone are not sufficient to integrally describe the overall behaviour of the system; however, under the framework of the presented theory such kinds of complex response are naturally revealed.

References

Arnol'd, V.I., 1975. Critical points of smooth functions and their normal forms. Russ. Math. Surveys 30 (5), 1–75.

Boal, D., 2002. Mechanics of the Cell. Cambridge University Press, Cambridge.

Connelly, R., Back, A., 1998. Mathematics and tensegrity. Am. Sci. 86, 142–151.

Coughlin, M.F., Stamenović, D., 1997. A tensegrity structure with buckling compression elements: application to cell mechanics. ASME J. Appl. Mech. 64, 480–486.

Coughlin, M.F., Stamenović, D., 1998. A tensegrity model of the cytoskeleton in spread and round cells. ASME J. Biomech. Eng. 120, 770–777.

Fuller, R.B., 1961. Tensegrity Portf. Artnews Ann. 4, 112–127.

Gilmore, R., 1981. Catastrophe Theory for Scientists & Engineers. Wiley, New York.

Golubitsky, M., Stewart, I., Schaeffer, D.G., 1988. Singularities and Groups in Bifurcation Theory, vol. II, Springer, New York (Appl. Math. Sci. 69).

Ingber, D.E., 1993. Cellular tensegrity: defining new rules of biological design that govern the cytoskeleton. J. Cell. Sci. 104, 613–627.

Ingber, D.E., 1998. The architecture of life. Sci. Am. 248 (1), 75–83.

Ingber, D.E., 2008. Tensegrity-based mechanosensing from macro to micro. Prog. Biophys. Mol. Biol. 97 (2–3), 163–179.

Ingber, D.E., Jamieson, J.D., 1985. Cells as tensegrity structures: architectural regulation of histodifferentiation by physical forces transduced over basement membrane. In: Andersson, L.C., Gahmberg, C.G., Ekblom, P. (Eds.), Gene Expression During Normal and Malignant Differentiation. Academic Press, Orlando, FL, pp. 13–32.

Ingber, D.E., Madri, J.A., Jamieson, J.D., 1981. Role of basal lamina in neoplastic disorganization of tissue architecture. Proc. Natl. Acad. Sci. USA 78, 3901–3905.

Kamm, R.D., Mofrad, M.R.K., 2006. Introduction, with the biological basis for cell mechanics. In: Mofrad, M.R.K., Kamm, R.D. (Eds.), Cytoskeletal Mechanics: Models and Measurements. Cambridge University Press, Cambridge, pp. 1–17.

Kenner, H., 1976. Geodesic Math and How to Use It? University of California Press, Berkeley.

Lanczos, C., 1977. The Variational Principles of Mechanics. University of Toronto Press, Toronto.

Lazopoulos, K., 1994. Location of bifurcation points and branching analysis in generalized coordinates. In: Papadrakakis, M., Topping, B.H.V. (Eds.), Advances in Computational Analysis. Civil Computation Ltd., Edinburg, Scotland, pp. 41–44.

Lazopoulos, K.A., 2005a. Stability of an elastic tensegrity structure. Acta Mech. 179 (1–2), 1–10.

Lazopoulos, K.A., 2005b. Stability of an elastic cytoskeletal tensegrity model. Int. J. Solids Struct. 42, 3459–3469.

Lazopoulos, K.A., 2006. On discontinuous strain fields in incompressible finite elastostatics. Int. J. Solids Struct. 43, 4357–4369.

Lazopoulos, K.A., Lazopoulou, N.K., 2006a. Stability of a tensegrity structure: application to cell mechanics. Acta Mech. 182, 253–263.

Lazopoulos, K.A., Lazopoulou, N.K., 2006b. On the elastica solution of a tensegrity structure: application to cell mechanics. Arch. Appl. Mech. 75, 289–301.

Lazopoulos, K.A., Markatis, S., 1994. On the singularities of constrained elastic systems – umbilics. Thin Wall. Struct. 19, 181–195.

Motro, R., 1992. Tensegrity systems: the state of art. Int. J. Space Struct. 7 (2), 75–83.

Ogden, R.W., 1997. Non-Linear Elastic Deformations. Dover, New York.

Pignataro, M., Luongo, A., 1994. Interactive buckling of an elastically restrained truss structure. Thin Wall. Struct. 19, 197–210.

Pirentis, A.P., Lazopoulos, K.A., 2006. On the elastica solution of a T3 tensegrity structure. Arch. Appl. Mech. 76 (7–8), 481–496.

Porteous, I.R., 1971. The normal singularities of a submanifold. J. Diff. Geom. 5, 543–564.

Porteous, I.R., 1994. Geometric Differentiation (For the Intelligence of Curves and Surfaces). Cambridge University Press, Cambridge.

Rivlin, R.S., 1948. Large elastic deformations of isotropic materials. II. Some uniqueness theorems for pure homogeneous deformation. Philos. Trans. R. Soc. Lond. Ser. A 240, 491–508.

Rivlin, R.S., 1974. Stability of pure homogeneous deformations of an elastic cube under dead loading. Q. Appl. Math. 32, 265–271.

Roth, B., Whiteley, W., 1981. Tensegrity frameworks. Trans. Am. Math. Soc. 265, 419–446.

Skelton, R.E., Helton, J., Adhikari, R., Pinaud, J., Chan, W., 2002. An Introduction to the Mechanics of Tensegrity Structures. CRC Press, Boca Raton, FL (Chapter 17).

Stamenović, D., 2006. Models of cytoskeletal mechanics based on tensegrity. In: Mofrad, M.R.K., Kamm, R.D. (Eds.), Cytoskeletal Mechanics: Models and Measurements. Cambridge University Press, Cambridge, pp. 103–128.

Stamenović, D., 2008. Cytoskeletal mechanics in airway smooth muscle cells. Resp. Physiol. Neurobiol. 163 (1–3), 25–32.

Stamenović, D., Coughlin, M.F., 1999. The role of prestress and architecture of the cytoskeleton and deformability of cytoskeletal filaments in mechanics of adherent cells: a quantitative analysis. J. Theor. Biol. 201, 63–74.

Stamenović, D., Fredberg, J.J., Wang, N., Butler, J.P., Ingber, D.E., 1996. A microstructural approach to cytoskeletal mechanics based on tensegrity. J. Theor. Biol. 181, 125–136.

Suresh, S., 2007. Biomechanics and biophysics of cancer cells. Acta Biomat. 3, 413–438.

Thom, R., 1975. Structural Stability and Morphogenesis. Benjamin/Addison-Wesley, New York/Reading, MA.

Thompson, J.M.T., Hunt, G.W., 1973. A General Theory of Elastic Stability. Wiley, New York.

Troger, H., Steindl, A., 1991. Nonlinear Stability and Bifurcation Theory. Springer, Wien.

Vainberg, M.M., Trenogin, V.A., 1974. Theory of Branching Of Solutions Of Non-Linear Equations. Noordhoff, Leiden (English translation).

Volokh, K.Yu., Vilnay, O., Belsky, M., 2000. Tensegrity architecture explains linear stiffening and predicts softening of living cells. J. Biomech. 33, 1543–1549.

Wang, N., Stamenović, D., 2000. Contribution of intermediate filaments to cell stiffness, stiffening and growth. Am. J. Physiol. Cell Physiol. 279, C188–C194.

Wang, N., Naruse, K., Stamenović, D., Fredberg, J.J., Mijailovich, S.M., Tolić-Nørrelykke, I.M., Polte, T., Mannix, R., Ingber, D.E., 2001. Mechanical behavior in living cells consistent with the tensegrity model. Proc. Natl. Acad. Sci. USA 98, 7765–7770.

Wendling, S., Oddou, C., Isabey, D., 1999. Stiffening response of a cellular tensegrity model. J. Theor. Biol. 196, 309–325.

Williams, W.O., 2007. A primer on the mechanics of tensegrity structures. Available from: <http://www.math.cmu.edu/users/wow/papers/newprimer.pdf>.